Design of Airfoils and Cascades of Airfoils

Theodosios P. Korakianitis*
Massachusetts Institute of Technology, Cambridge, Massachusetts

This paper presents a method for generating blade shapes to be used as inputs to the direct- or inverse-blade-design sequences. This method can generate subsonic or supersonic blades for compressors and turbines, or isolated airfoils, but the discussion in this paper is limited to subsonic-exit turbine blade rows. Gas-turbine blades are usually designed by a mixture of iterative, direct- and inverse-blade-design methods. The iterations are enormously reduced if the initial blade shape has performance characteristics near the desirable ones. The desirable performance characteristics are presented, and ways to manipulate the input striving for such characteristics (minimizing design iterations) are discussed. The overspeed regions near the leading edge are avoided. The performance curves of three blades generated by this method are included. It is concluded that blade performance is extremely sensitive to small changes in the shape of the surfaces and to changes or discontinuities in the derivative of the curvature of the blade surfaces. The order of magnitude of these changes is the same or lower than the order of magnitude of the thickness distribution of the boundary layers.

Nomenclature

a	= coefficient of thickness distributions
b	= axial chord length
$b1c$	= angle of construction line at the origin
C	= chord length
M	= Mach number
p	= pressure
S	= tangential spacing of the blades
x,y	= coordinates
yp	= line segment on the pressure surface
ys	= line segment on the suction surface
XP, YP	= point on the pressure surface of the blade
XS, YS	= point on the suction surface of the blade
tpr	= pressure side root-x coefficient
tsr	= suction side root-x coefficient [Eq. (3)]
α	= flow angle
β	= angle of the blade surface (see Fig. 2)
$\beta 1c$	= angle of construction line at the origin
λ	= stagger angle of the blade
τ	= thickness distribution near the leading edge

Subscripts

$0,1,2,\ldots$	= with XP, YP, XS, and YS points on the blade
$0,1,2,3$	= with yp and ys, line segment on the blade
$1,2$	= with flow angle or Mach number, inlet and outlet, respectively
c	= construction line
p	= pressure side
rb	= rotor-blade cascade
s	= suction side

Introduction

GAS-turbine blades are three-dimensional objects operating in a complex flowfield. Because of its complexity, the problem usually is reduced to a series of two-dimensional problems (solved for some diameters). Blade design is partly a science and partly an art. The performance of the blades is expressed in the form of some property distribution (such as pressure, velocity, etc.) on the blade surface and in the cascade passage. Two-dimensional designs are "stacked" using some rules for the locus of the centers of areas of the sections and the three-dimensional shape of the leading edge and of the trailing edge. Compromises in performance must be made to accommodate these three-dimensional constraints.

Blade cascades can be designed by direct or inverse methods. In the direct method the designer inputs the geometry of the blade, and the output is the performance of the airfoil. The blade geometry is modified until a desirable performance is obtained. In the inverse method the designer usually starts from some initial blade shape and performance, and inputs the desired modifications to the performance. The output is a new shape and its performance, which is as close to the desired (input) performance as permitted by the equations modeling the flow. Both methods are iterative and are based on the assumption of steady-inflow and steady-outflow conditions (although the flow around the blades during engine operation is inherently unsteady).

Both methods have relative advantages and disadvantages. The direct method is laborious; it requires considerable insight and many iterations until an acceptable performance is obtained. On the other hand, the designer has direct control of the various geometric parameters, and infeasible blade shapes are excluded before they are analyzed. The inverse method is less laborious, but must start from the direct method anyway. The designer has less control on the blade shape and on the resulting performance. The resulting blade shape may be infeasible due to stress considerations. If one decides that some geometric parameters (such as the stagger angle) must be changed, one must start from the direct method again.

The final design is usually obtained by a judicious combination of both methods, although if an inverse method is not available, one could use the direct method exclusively. In any case, one would like to start the inverse method with a blade shape close to an acceptable design, since this will reduce enormously the number of inverse-design iterations. The purpose of this paper is to provide a design tool for generating initial blade shapes for either method.

Background

Gas-turbine-blade cascades operate in an inherently unsteady environment. The flow is affected by viscosity,

Received April 14, 1987; presented as Paper 87-2171 at the AIAA/SAE/ASME/ASEE 23rd Joint Propulsion Conference, San Diego, CA, June 29–July 2, 1987; revision received Oct. 16, 1987.

*Graduate Research Assistant, Department of Mechanical Engineering; currently Assistant Professor, Department of Mechanical Engineering, Washington University, St. Louis, MO. Member AIAA.

wakes, potential interaction, vortex generation, turbulence, three-dimensional effects such as radial components of velocity, end-wall effects, leakage flows, and the interaction of the above. Demands for improvements in performance and reduction of engine weight and cost have led to increases in temperature, which add the effect of cooling flows, and have led to increases in loading, which make good performance harder to obtain. These demands require sophisticated methods for blade design because the performance of the airfoils becomes critical. Because of the lack of methods that can take into account all of these effects, blades are designed for steady-inflow and steady-outflow conditions. With current technology, we are still a long way from a blade-design method that incorporates the effects of unsteadiness in the early blade-design sequence.

This work was initiated by the need for a series of typical, modern turbine blades on which to study the effects of unsteady flow on the generation of unsteady forces on gas-turbine blades.[1,2] Engine manufacturers do not publish the geometry of the blade shapes they develop. Thus, we needed to design our own blade series for the aforementioned work.

The blade-design sequence depends on the application and on the global constraints of the engine. Design sequences are described in some texts (for examples, see Refs. 3 and 4). The designer has many choices, but for the purposes of this paper we will refer to the diagram of Fig. 1, and we will assume that the designer has chosen the velocity diagram (and, hence, the inlet flow angle α_1 and outlet flow angle α_2 of the cascade) and the exit Mach number M_2 in the absolute frame for stators and in the relative frame for rotors. Three additional choices must be made: some specification for the tangential spacing S between the blades, some specification for the inclination of the blades with respect to the axial direction x, and the trailing-edge thickness.

The spacing between the blades (which is directly linked to the number of blades in the blade row) is a function of the tangential lift coefficient C_L and is defined by

$$C_L \equiv \frac{\text{tangential aerodynamic force}}{\text{tangential blade area} \times \text{outlet dynamic head}} \tag{1}$$

This expression can be manipulated in a number of ways (for compressible flow, for incompressible flow, accounting for variations in axial-flow velocity, etc.). Here we chose the incompressible-flow derivation (see Ref. 3), which reduces C_L to

$$C_L = 2S\cos^2\alpha_2(\tan\alpha_1 - \tan|\alpha_2|)/b \tag{2}$$

The stagger angle λ is defined as the angle between the line joining the leading-edge point and the trailing-edge point on the pressure surface, and a line in the axial direction. Suggested values for the stagger angle have been published by Kacker,[5] although the designer has considerable flexibility in specifying the stagger angle, and different methods are used in various companies. The trailing-edge thickness is controlled by the amount of cooling air and by considerations of structural integrity.

The outlet flow angle α_2 depends on the throat diameter o. The latter is a critical parameter that affects the whole design. The industry has for years depended on the Ainley-Mathieson method[6] and on improvements to it (e.g., by Dunham[7]) for the prediction of the outlet flow angle as function of exit Mach number, spacing, and throat diameter. This is sufficient for preliminary design. Today's computer programs (such as ISES[8]) are more accurate and compute the outlet flow angle. Gostelow[9] has explained how the result depends not only on the geometry but also to some extent on the Kutta condition at the trailing edge.

Method

Early blade-design methods were based on the distribution of a specified thickness function around a camber line. Examples of such methods have been published by Dunham,[10] and earlier methods have been included in pages 7–11 of the text by Moran.[11] These methods do not provide enough flexibility to control both the suction and pressure surfaces in order to obtain a desirable performance. In modern methods each surface is varied independently.

The method described in this paper is based on specifying five points (excluding the trailing-edge points and the origin) and two slopes on each surface and on generating the leading-edge region with two thickness distributions added perpendicularly to two parabolic construction lines (see Fig. 2). The two-dimensional Cartesian coordinates of the five points on the suction surface are (XS_0, YS_0), (XS_1, YS_1), (XS_2, YS_2), (XS_3, YS_3), and (XS_4, YS_4); and the corresponding points on the pressure surface are (XP_0, YP_0), (XP_1, YP_1), (XP_2, YP_2), (XP_3, YP_3), and (XP_4, YP_4). In the following sample blades, the x locations of these points have been kept constant at axial-chord positions 0.10, 0.20, 0.40, 0.60, and 0.80. Also, the blades are generated with pointed trailing edges because they have been analyzed using incompressible calculation methods, and they are assumed to include the effects of boundary-layer blockage to the flow. This means that the shapes shown are the outside surfaces of the boundary layers developed around the airfoils, and that the trailing edge includes a computational "cusp." The inlet flow angle α_1, the outlet flow angle α_2, and the loading coefficient C_L specify the tangential spacing S between the blades for unit axial chord b [see Eq. (2)]. The stagger angle specifies the location of the trailing-edge point (1.00, $\tan\lambda$). If a trailing-edge thickness is desired, one can add a parameter and displace the two trailing-edge points by the trailing-edge thickness or a circular arc of specified radius, and use viscous calculation methods. The trailing-edge blade angle is specified by the two slopes of the suction and pressure surfaces at the trailing edge, β_{s2} and β_{p2}, respectively. Since this trailing edge is where the suction and pressure boundaries "collapse," the trailing-edge angle specified here is smaller than that of the blade material. Two corresponding points and slopes are defined near the leading edge. The slope of the suction surface at point (XS_0, YS_0) is β_{s1}, and the slope of the pressure surface at point (XP_0, YP_0) is β_{p1}. In addition, two parabolic construction lines are specified: one for the suction surface and one for the pressure surface. The suction-side construction line passes through points

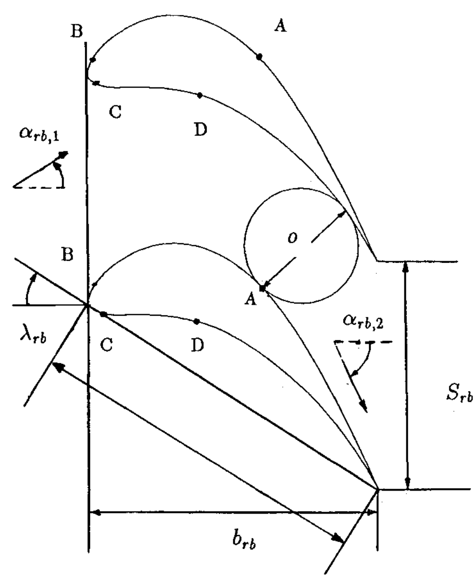

Fig. 1 Geometry of a typical cascade.

(0.0, 0.0) and (XS_c, YS_c) and has slope $\beta 1c_s$ at the origin. The pressure-side construction line passes through points (0.0, 0.0) and (XP_c, YP_c) and has slope $\beta 1c_p$ at the origin. In the sample blades shown in this paper, $XP_c = XS_c = 0.20$. The program that generates the geometric shapes of the blades permits altering the values of all these x locations, but for the blade shapes to be discussed here, it was found that it was not necessary to use other x locations for the points on the surfaces.

Sample inputs are shown in Table 1. Although 34 parameters are shown, some of the parameters have been standardized (as mentioned above), and 23 of those are actively used. After the first few trials, only one or two of these parameters are actually manipulated at a time, until a desirable shape is obtained.

Each surface is developed separately by four adjoining lines. The development of the suction surface is discussed for illustration. The development of the pressure surface is similar to that of the suction surface. The section of the suction surface ys_1 between $x = XS_0$ and $x = XS_2$ is a linear third-order polynomial that passes through points (XS_0, YS_0), (XS_1, YS_1), and (XS_2, YS_2) and has the specified slope β_{s1} at the first point. The section of the suction surface ys_3 between $x = XS_3$ and $x = 1.0$ is a linear third-order polynomial that passes through points (XS_3, YS_3), (XS_4, YS_4), and (1.00, tanλ) and has the specified slope β_{s2} at the last point. The section of the suction surface ys_2 between $x = XS_2$ and $x = XS_3$ is a linear fifth-order polynomial that passes through points (XS_2, YS_2) and (XS_3, YS_3) and matches first and second derivatives with lines ys_1 and ys_3 at the adjoining points. When the blade geometry is close to a desirable shape, ys_2 is changed into a linear seventh-order polynomial that, in addition to the previous conditions, matches the slopes of the curvatures of the lines ys_1, ys_2, and ys_3 at points (XS_2, YS_2) and (XS_3, YS_3). The portion of the suction surface between the origin and point (XS_0, YS_0) is a line ys_0 derived from a thickness distribution added perpendicularly above the suction-side construction line. This thickness distribution is of the form

$$\tau = tsr \cdot \sqrt{x} + a_{s1} \cdot x + a_{s2} \cdot x^2 + a_{s3} \cdot x^3 + a_{s4} \cdot x^4 \tag{3}$$

where tsr is an input parameter (see Table 1), and the coefficients a_{s1}, a_{s2}, a_{s3}, and a_{s4} are derived with the conditions that the absolute value, first and second derivatives, and the slopes of the curvatures of lines ys_0 and ys_1 with respect to the parabolic construction line are equal at point (XS_0, YS_0).

The iterations begin by designing the surfaces between $x = XS_0$ and $x = 1.00$. The first step is to specify the stagger angle λ and the slopes of the surfaces near the trailing edge and at $x = XS_0$, then evaluate the required throat diameter o, and next specify the points around the two surfaces in such a way as to ensure that the throat has the required value of o. Alternatively, the point of tangency of the throat diameter with the suction line can become an input parameter with small modifications to the method. To avoid recompression, the area along the passage should be continuously decreasing. For the subsonic cascades studied here, the slope at the suction-side trailing edge should be slightly lower (negative values by 1-2 deg) than the required outlet flow angle, and that of the pressure side should be slightly higher (by 2-4 deg) than the required outlet flow angle. A suggested range of values for the angle between the suction- and the pressure-surface lines at $x = 0.90$ is 5-10 deg. Another parameter is the amount of turning of the suction surface in the region of unguided diffusion, which is the length of the blade on the suction surface from the throat to the trailing edge. A suggested range of values for this angle is 10-18 deg.

With this method, the foremost point of the blade may have a value that is less than zero, which means that the blade spacing must be recalculated for the new axial blade chord (larger than 1.00) using Eq. (2). If it appears that even with relatively flat (low curvature) surfaces the leading edge is below the origin, then the stagger angle is too low (negative values). The value of the stagger angle dictates the distribution of the turning of the flow along the passage and the distribution of aerodynamic loading along the blade. The philosophy of favoring forward or aft turning and loading of the blades varies from company to company. If it appears impossible to achieve a continuous reduction in area from upstream to downstream, even for relatively thin blades, then the stagger angle is too high.

When the resulting blade surfaces are smooth to the eye, finer adjustments should be made [by small changes in the y

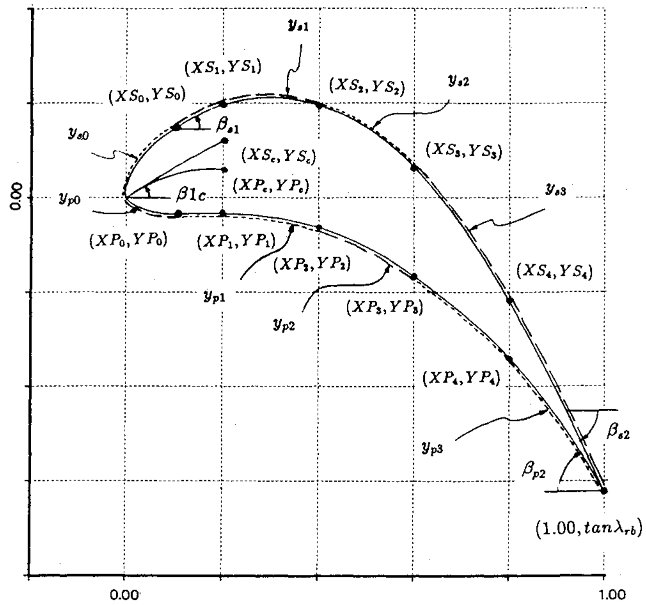

Fig. 2 Parameters defining the blade.

Table 1 Parameters specifying the blades

Parameter	4060c10	3070c08	3070c10
α_1	40	30	30
α_2	−60	−70	−70
C_L	1.00	0.80	1.00
λ	−32.00	−44.00	−46.00
$\beta 1c_s$	35.00	50.00	30.00
XS_c	0.1000	0.2000	0.2000
YS_c	0.0650	0.1500	0.1155
YS_0	0.1476	0.2340	0.2200
β_{s1}	33.50	32.00	35.74
β_{s2}	−65.70	−74.00	−72.36
XS_1	0.2000	0.2000	0.2000
YS_1	0.1965	0.2800	0.2684
XS_2	0.4000	0.4000	0.4000
YS_2	0.1956	0.2800	0.2308
XS_3	0.6000	0.6000	0.6000
YS_3	0.0664	0.1180	0.0059
XS_4	0.8000	0.8000	0.8000
YS_4	−0.2200	−0.3200	−0.4448
tsr	0.1300	0.3000	0.1000
$\beta 1c_p$	35.00	35.00	30.00
XP_c	0.1000	0.2000	0.2000
YP_c	0.0500	0.0700	0.0700
YP_0	−0.0350	−0.0200	−0.0120
β_{p1}	2.00	1.00	0.00
β_{p1}	−61.00	−68.00	−67.00
XP_1	0.2000	0.2000	0.2000
YP_1	−0.0340	−0.0200	−0.0230
XP_2	0.4000	0.4000	0.4000
YP_2	−0.0635	−0.0650	−0.1000
XP_3	0.6000	0.6000	0.6000
XP_3	−0.1660	−0.2150	−0.2681
XP_4	0.8000	0.8000	0.8000
YP_4	−0.3400	−0.5200	−0.6000
tpr	0.3000	0.1500	0.3000

values of the (x,y) points] while evaluating the first derivative of the blade surfaces, which should be smooth. The next step is to evaluate the curvature of the blade surfaces, which *must* be smooth. Since the pressure and corresponding velocity around the blades are a function of curvature, local maxima and minima of the curvature will be reproduced on the velocity distribution. This may lead to the formation of local separation bubbles at regions of deceleration, which are detrimental to performance. The above specification of the blade surfaces is such that the curvature along the blade surfaces is continuous, but local maxima or minima of the curvature (discontinuities in the slope of the curvature) affecting the performance may occur at or between $x=0.40$ and $x=0.60$ when ys_2 is a fifth-order rather than a seventh-order polynomial. These can be smoothed by small changes in the y locations at these points and by small changes in the slopes at $x=XS_0$ and $x=1.00$, and later fine-tuned (by changing the specification of line ys_2 to seventh-order polynomial and by manipulating the values of *tsr* and *tpr*). The flow is usually continuously accelerating on the pressure surface, and the Mach numbers in this region are low. Local maxima and minima of the curvature should be smoothed on the pressure surface but eliminating them fully is essential only when heat-transfer considerations are dominant (for example in turbine blades). Contrary to that, local maxima and minima on the curvature of the suction surface must be smoothed because they are reproduced on the velocity distribution of that surface. The velocity and pressure distributions at this region of the suction surface are very critical because they occur at the throat, near the throat, or in the region of unguided diffusion for most designs, where the Mach numbers are relatively high.

Since the thickness distributions are added perpendicularly to the construction lines, specifying $b1c_s = b1c_p$ will ensure that the leading edge has a smooth transition between the suction and pressure sides. The value of this angle should be near the inlet flow angle (± 10 deg), but the exact value depends on the shape of the individual blade. The parameters *tsr* and *tpr* can have different values, and the points (XP_c, YP_c) and (XS_c, YS_c) do not need to coincide. This approach is more flexible than the usual "leading-edge wedge angle" and "leading-edge circle" because it enables optimization of the shape in the regions of diffusion that may occur near the leading edge on both sides of the airfoil. Inverse-design methods have difficulty dealing with points near the leading edge, and overspeed regions due to the leading-edge circle are difficult to correct.

Performance Characteristics

The objective of the airfoil is to generate lift by curving the flow while minimizing losses. Losses are generated by the imbalance of pressure at inlet and exit (profile or form drag) and by shear forces between the fluid and the airfoil (skin-friction drag). Both forms of drag are generated by the presence of boundary layers around the blades. Therefore, the performance characteristics of blades must be examined while estimating the effects of the flowfield on the boundary layers. Predictions of this sort are difficult because the Reynolds numbers in turbine blades are in the regions of transition between laminar and turbulent boundary layers. The nature of the boundary layer depends on surface roughness and curvature, freestream turbulence, and the local effects of two-dimensional and three-dimensional disturbances. The presence of laminar or turbulent boundary layers affects the shape of the outer layer of the displacement thickness, the nature of the reattachment, the length and shape of the separation bubbles, and the heat-transfer characteristics, which radically change the demands on cooling flows and, thus, on the shape of the airfoils around the leading and trailing edges. There are also three-dimensional effects generated by radial redistribution of flow and three-dimensional effects due to the passage vortex (created by the turning of vorticity generated by end-wall boundary layers at the inlet). The above are unsteady effects generated in steady flow. In addition, there are unsteady effects due to impingement of wakes and vortices from upstream blade rows and due to potential interaction effects between neighboring blade rows.

These phenomena (especially the three-dimensional effects of secondary flows) are not all very well understood to date, but treatises on them have been published by Gostelow[12] and Sieverding,[13] while supporting experimental results have been published by Sharma,[14] Han,[15] Hodson,[16] Roberts,[17] Hourmouziadis,[18] and others. Blade design is affected in three major ways by the development of the boundary layer. First, in the region of unguided diffusion there is an adverse pressure gradient on the suction side that induces separation near point A in Fig. 1.[18] Second, on both sides of the leading edge there may be a region of sharp change of curvature where the leading-edge circle blends with the two surfaces near points B and C in Fig. 1, which are called overspeed regions and may induce separation bubbles.[16] Third, depending on the shape of the pressure surface, there may be a diffusing region between points C and D in Fig. 1. The blade-design method presented here deals in an optimal fashion with the problem at all these points. At points B and C there is no blending with a leading-edge circle and the designer can control the curvature by varying the input until the curvature of the surfaces are smooth. The five points that control the shape of the pressure surface provide enough flexibility for the control of the expansion better than other methods (for example, the third-order polynomial suggested by Pritchard[19]). If after the first direct-method calculation it is found that there is indeed diffusion near point D or between points C and D, then the points controlling the surface must be lowered to eliminate the problem. Finally, the problem at point A can be minimized by careful control of the curvature in that region (but the adverse pressure gradient and the unguided diffusion are characteristics of the passage and cannot be eliminated entirely). One frequently used parameter here is the ratio of the maximum flow velocity on the suction surface divided by the flow velocity at the trailing edge, which is called the diffusion ratio. For blade rows of low $C_L(<0.9)$ [see Eq. (2)] one should aim for diffusion ratios less than 1.25; for blade rows of high $C_L(>1.0)$, the diffusion ratio may be a little higher.

Sample Blades

The sample cases presented here have been designed for relative exit Mach number of 0.80, and they have been analyzed with the use of the steady-flow calculation of Giles' computer program UNSFLO.[20,21] (The blade-design method presented in this paper can be used to design blades that subsequently will be analyzed by any direct- or inverse-calculation method.) Since UNSFLO is currently an inviscid program, pointed trailing edges have been specified. The shapes analyzed are assumed to be the outside of the boundary-layer surfaces (with the displacement thickness), and the stagger angles are slightly higher than those suggested by Kacker.[5] In the following blade notation, the first two digits refer to the inlet flow angle in degrees, the next two digits refer to the outlet flow angle in degrees, and the last two digits (separated by a "c" from the first four) refer to the tangential-lift coefficient given by Eq. (2). For example, blade 4060c10 refers to a blade with inlet flow angle of 40 deg, outlet flow angle of 60 deg, and tangential-loading coefficient of 1.00. Table 1 gives the parameters that define (and can reproduce according to the method presented above) the geometry of the blades. The geometry and the performance of 13 blades have been included in Ref. 1 in this fashion. Similarly, the geometry and the performance of five of those blades have also been included in Ref. 22.

Figure 3 shows the curvature of the blade surfaces of the 4060c10 blade and another blade whose parameters are a little different (from $x=0.10$ to $x=1.00$). The differences between the two blades are so small that they can be seen only on enlargements of very small sections of the surfaces; they are well

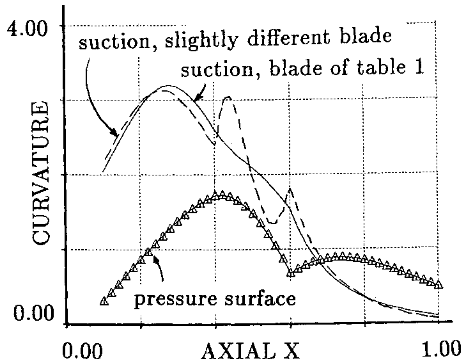

Fig. 3 Curvature of the surfaces of blade 4060c10.

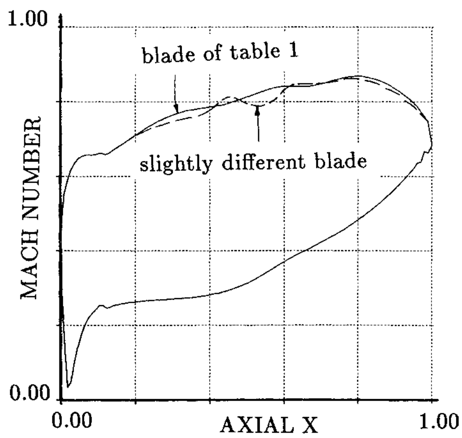

Fig. 4 Surface Mach number distribution of blade 4060c10.

within the order of magnitude of the boundary-layer displacement thickness. The solid lines correspond to the parameters of the blade shown in Table 1. The surface Mach number distributions are shown in Fig. 4. There is a direct correspondence between the shape of the curvature and the shape of the Mach number distribution (which was expected, since the governing equations are a strong function of the local radius). The effect is more pronounced on the suction side because the Mach number is higher. The small discontinuities in Mach number distribution around $x=0.10$ can be smoothed by an inverse-design program, but the performance shown here is already satisfactory. The corresponding passage Mach number distribution (for the blade whose parameters are in Table 1) in increments of 0.05 is shown in Fig. 5.

Figure 6 shows the curvature of the blade surfaces of the 3070c08 blade. The corresponding surface Mach number distributions are shown in Fig. 7. Again, there is a direct correspondence between the shape of curvature and the shape of the Mach number distribution. In this blade there is some diffusion on the pressure surface (in the region between points C and D in Fig. 1). This situation would be improved by lowering the y values of the blade surfaces in that region. The corresponding passage Mach number distribution in increments of 0.05 is shown in Fig. 8.

The curvature of the suction surface of blade 3070c10 is similar to the solid line shown in Fig. 3 for blade 4060c10. The corresponding surface Mach number distribution of blade 3070c10 (solid line) and that of the same blade as modified after a few inverse-design iterations (broken line) are shown in Fig. 9. The program ISES, developed by Drela and Giles,[8] was used for the inverse-design calculations. The differences between the two blades are so small that they can be seen only on enlargements of very small sections of the surfaces. The corresponding passage Mach number distribution (for the blade

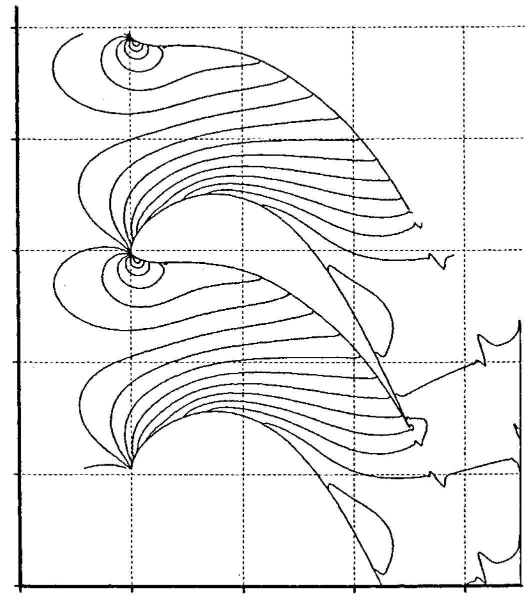

Fig. 5 Passage Mach number distribution of blade 4060c10 (Mach number increment of 0.05).

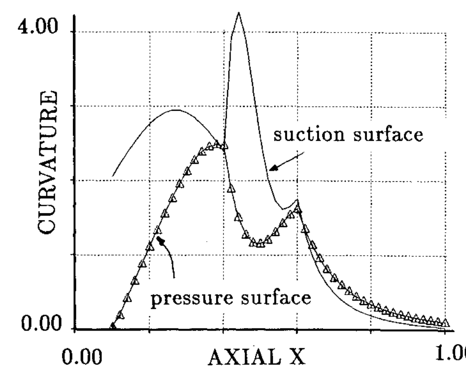

Fig. 6 Curvature of the surfaces of blade 3070c08.

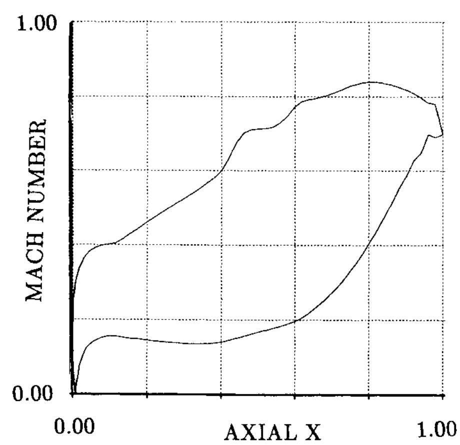

Fig. 7 Surface Mach number distribution of blade 3070c08.

whose parameters are shown in Table 1) in increments of 0.05 is shown in Fig. 10.

If the blades were designed for a higher exit Mach number, then the curvature of the suction surfaces near the trailing edges would be lower (flatter surface) for the same diffusion ratio. This would change accordingly the other parameters of the blade. For supersonic Mach numbers some back curvature may be required for acceptable performance.

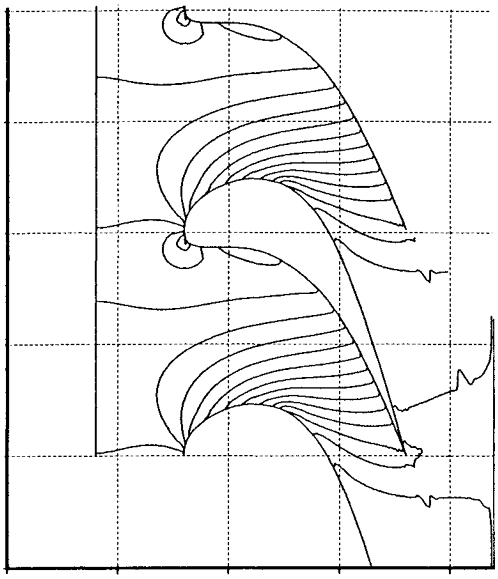

Fig. 8 Passage Mach number distribution of blade 3070c08 (Mach number increment of 0.05).

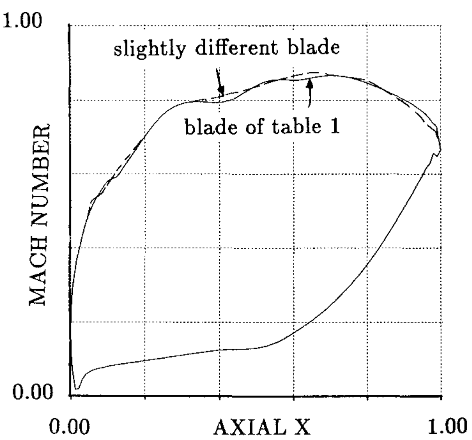

Fig. 9 Surface Mach number distribution of blade 3070c10.

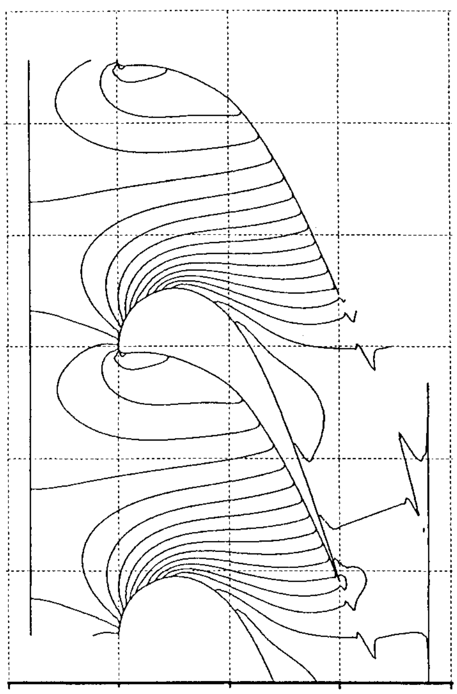

Fig. 10 Passage Mach number distribution of blade 3070c10 (Mach number increment of 0.05).

Conclusions

A new parametric blade-design method has been introduced. The method can be used to design subsonic or supersonic blades for compressors or turbines, or isolated airfoils, but the discussion in this paper is limited to subsonic-exit turbine blades. The blade shapes are specified by a few points and other geometric parameters on the blade surfaces. This method permits the user to specify the leading edge by two thickness distributions around two independent construction lines, thus avoiding the overspeed regions near the leading edge (because it does not employ the usual blending in of the curvatures near the leading-edge circle). The discontinuities in curvature occur at higher axial locations where they can be smoothed by iterations or by inverse design methods without affecting the performance in the leading-edge region. It is found that the blade performance, judged by the shape of the surface Mach number distribution, is very sensitive to changes in the slope of the curvature of the blades. The performance is extremely sensitive to small changes of the surface geometry (changes of smaller order of magnitude than the boundary-layer thickness or small erosion damage). Diffusion on the pressure side, if it occurs, can be eliminated by lowering the pressure side (thickening the blade in that region). The performance curves of three representative blades are used for discussion.

Acknowledgments

The material presented in this paper was part of a larger research program funded in part by the General Electric Company. The author wishes to thank Mr. Dennis C. Evans of the General Electric Company (Lynn, Massachusetts), and Professors David Gordon Wilson, A. D. Carmichael, Michael B. Giles, and Anthony T. Patera of MIT for their advice, support, encouragement, and constructive suggestions.

References

[1]Korakianitis, T. P., "A Design Method for the Prediction of Unsteady Forces on Subsonic, Axial Gas-Turbine Blades," Ph.D Dissertation (Sc.D.), MIT, Cambridge, MA, July 1987.

[2]Korakianitis, T. P. and Wilson, D. G., "On the Effect of the Magnitude of the Inlet-Boundary Disturbance on the Unsteady Forces on Axial Gas-Turbine Blades," *Proceedings of the 4th Symposium on Unsteady Aerodynamics and Aeroelasticity of Turbomachines and Propellers*, edited by H. E.Gallus and S. Seruaty, Feb. 1988, pp. 109–124.

[3]Wilson, D. G., *The Design of High-Efficiency Turbomachinery and Gas Turbines*, MIT Press, Cambridge, MA, 1984.

[4]Horlock, J. H., *Axial Flow Turbines*, Butterworths, London, 1966.

[5]Kacker, S. C. and Okapuu, U., "A Mean-Line Prediction Method for Axial-Flow Turbine Efficiency," American Society of Mechanical Engineers, New York, Paper 81-GT-58, 1981.

[6]Ainley, D. G. and Mathieson, G. C. R., "A Method of Performance Estimation for Axial-Flow Turbines," British Aeronautical Research Council, London, R&M 2974, 1951.

[7]Dunham, J. and Came, P. M., "Improvements to the Ainley-Mathieson Method of Turbine Performance Prediction," *Transactions of the ASME, Journal of Engineering for Power*, Ser. A, Vol. 92, July 1970, pp. 252–256.

[8]Drela, M. and Giles, M. B., "A Two-Dimensional Viscous Aerodynamic Design and Analysis Code," AIAA Paper 87-0424, 1987.

[9]Gostelow, J. P., "Trailing Edge Flows Over Turbomachine Blades and the Kutta-Joukowsky Condition," American Society of Mechanical Engineers, New York, Paper 75-GT-94, 1975.

[10]Dunham, J., "A Parametric Method of Turbine Blade Profile Design," American Society of Mechanical Engineers, New York, Paper 74-GT-119, 1974.

[11]Moran, J., *An Introduction to Theoretical and Computational Aerodynamics*, Wiley, New York, 1984.

[12]Gostelow, J. P., *Cascade Aerodynamics*, Pergamon, New York, 1984.

[13]Sieverding, C. H., "Recent Progress in the Understanding of Basic Aspects of Secondary Flows in Turbine Blade Passages," American Society of Mechanical Engineers, New York, Paper 84-GT-78, 1984.

[14]Sharma, O. P., Wells, R. A., Schlinker, R. H., and Bailey, D. A., "Boundary Layer Development on Turbine Airfoil Suction Surfaces," American Society of Mechanical Engineers, New York, Paper 81-GT-204, 1981.

[15]Han, L. S. and Cox, W. R., "A Visual Study of Turbine Blade Pressure-Side Boundary Layers," American Society of Mechanical Engineers, New York, Paper 82-GT-47, 1982.

[16]Hodson, H. P., "Boundary-Layer Transition and Separation Near the Leading Edge of a High-Speed Turbine Blade," American Society of Mechanical Engineers, New York, Paper 84-GT-179, 1984.

[17]Roberts, G. and Brown, A., "Boundary-Layer Transition Regions on Turbine Blade Suction Surfaces," American Society of Mechanical Engineers, New York, Paper 84-GT-284, 1984.

[18]Hourmouziadis, J., Buckl, F., and Bergmann, P., "The Development of the Profile Boundary Layer in a Turbine Environment," *Transactions of the ASME, Journal of Turbomachinery*, Vol. 109, No. 2, April 1987, pp. 286–295 (American Society of Mechanical Engineers, New York, Paper 86-GT-244, 1986).

[19]Pritchard, L. J., "An Eleven Parameter Axial Turbine Airfoil Geometry Model," American Society of Mechanical Engineers, New York, Paper 85-GT-219, 1985.

[20]Giles, M. B., "Calculation of Unsteady Wake/Rotor Interactions," AIAA Paper 87-0006, 1987.

[21]Giles, M. B., "UNSFLO: A Numerical Method for Calculating Unsteady Stator/Rotor Interaction," MIT Computational Fluid Dynamics Lab., Cambridge, MA, TR-86-6, 1986.

[22]Korakianitis, T. P., "A Parametric Method for Direct Gas-Turbine-Blade Design," AIAA Paper 87-2171, June 1987.